Polymer Vol. 39 No. 16, pp. 3871–3875, 1998

0032-3861/98/$19.00+0.00

PII: S0032-3861(97)10218-X

polymer communications

Silicon nitride membrane substrates for the investigation of local structure in polymer thin films

T. L. Morkved[a], W. A. Lopes[a], J. Hahm[b], S. J. Sibener[b] and H. M. Jaeger[a,*]
[a]*Department of Physics, The James Franck Institute, The University of Chicago, 5640 S. Ellis Ave., Chicago, IL 60637, USA*
[b]*Department of Chemistry, The James Franck Institute, The University of Chicago, 5640 S. Ellis Ave., Chicago, IL 60637, USA*
(Received 16 May 1977; accepted 10 October 1997)

The fabrication of silicon nitride membrane substrates and their use in studies of polymer thin films are described. As an integral part of a wafer, these membranes are both self-supporting and transparent for transmission electron microscopy (TEM). Therefore, the same polymer film can be spin-cast on the substrate and, without being removed, studied by a variety of techniques, including TEM, and atomic force microscopy (AFM). To demonstrate the utility of these substrates in characterizing both global and local film morphology, experimental results are presented on polystyrene–polymethylmethacrylate diblock copolymers in the ultrathin film limit, using optical microscopy together with combinations of AFM and TEM at the same location. The addition of microfabricated structures to these substrates, such as planar electrodes is also discussed. © 1998 Published by Elsevier Science Ltd. All rights reserved.

(Keywords: thin film morphology; silicon nitride membrane substrates; block copolymers)

Introduction

Over the past few years much interest has focused on the investigation of polymer thin films, both because of their tremendous technological importance and because of their potential for novel behavior not found in bulk[1]. As the film thickness is decreased, the influence of the interfaces at either film surface becomes more prominent and surface wetting effects often determine the film properties and structure. This is of particular consequence for polymer blends and copolymer melts where microphase separation in the presence of such interfaces can lead to morphologies that are unique to thin films. A wide range of experimental techniques are available to probe both the local and the large-scale structure of polymer thin films[1], including optical[2], ion[3] and electron microscopy[4,5], neutron[6] and X-ray scattering[3], and various scanning probe microscopies[7]. In many ways, these techniques are complimentary and become most powerful when used in combination. However, most of them traditionally involve specific sample preparation techniques that are incompatible. For example, spin-casting, a standard method for preparing thin films of highly uniform thickness, requires a solid substrate as support. Such substrates prohibit direct imaging of the local film morphology by transmission electron microscopy (TEM) without first removing[4] or microtoming the film[5]. Conversely, many of the traditional thin film preparation techniques such as microtoming, droplet casting, or spin-casting on dissolvable substrates such as NaCl are well-suited for TEM investigations of local structure, but cannot easily be combined with other techniques such as scattering techniques or scanning probe microscopy without remounting the film. Furthermore, they also cannot be integrated with modern microfabrication methods which typically require a solid substrate. Such integration is highly desirable, however, because microlithographically patterned substrates can induce new spatial properties in polymer thin films by utilizing commensurability or confinement effects[8], by area-specific wetting[9], or by electric field orientation[10].

Here we present the use of silicon nitride substrates as a means to overcome some of these obstacles. These substrates consist of a thin (typically 100 nm) layer of amorphous, low-stress silicon nitride grown onto a silicon wafer. Direct imaging of the local polymer morphology requires a substrate transparent to an electron beam. Therefore, a number of small areas of the wafer were lithographically patterned and etched away from the wafer's backside, producing silicon nitride membrane 'windows' with typical dimensions ranging from 60 to 300 μm (see *Figure 1*). These membranes are self-supporting and integral to the wafer surface which thus consists of a smooth, contiguous silicon nitride layer. Polymer thin films can be spin-cast onto these substrates with the high degree of control and reliability known from spinning on solid Si wafers. The substrates are inert, easily withstand typical polymer annealing conditions, and allow for microlithographic patterning by standard methods. In this paper we demonstrate how these features allow for measurements by optical microscopy, ellipsometry, AFM, and TEM all on the same film area without the need to remove the sample. The examples chosen focus on results we obtained for polystyrene–polymethylmethacrylate diblock copolymer (PS-b-PMMA) films. However, the techniques used should be applicable for almost any type of thin organic film.

Silicon nitride membrane fabrication

Silicon nitride membranes are commonly used for a variety of applications too numerous to list here, ranging from vacuum windows[11] to substrates for aperture

* To whom correspondence should be addressed

fabrication[12], and have been used recently to study magnetic films using combined TEM and magnetic force microscopy[13]. The fabrication process follows standard procedures which we summarize below. Both sides of double-side-polished, 0.25 mm thick, ⟨100⟩ silicon wafers are prepared by stripping the oxide layers. Amorphous, low stress silicon nitride is then deposited via low pressure chemical vapor deposition onto both sides. On the backside, standard photolithography is used to pattern rectangular openings into photoresist which serve as templates for the membranes. The openings are aligned with their sides parallel and perpendicular to the wafer's ⟨110⟩ crystal axis. Inside the openings, the silicon nitride is removed by reactive ion etching with CF_4, and then the remaining photoresist is removed. The underlying, exposed silicon is then etched with an aqueous KOH solution at 90°C, which etches the (100) and (110) planes of crystalline silicon faster then the (111) planes. This anisotropic etch, which creates an etch profile that makes an angle of 54.7° with respect to the wafer surface[14], etches through the silicon wafer but stops at the silicon nitride on the front side of the wafer, producing membranes whose size is determined mainly by geometry and the size of the starting hole. Finally, a short isotropic etch is used to complete the procedure. For easy partitioning of a large wafer into individual substrates, additional scribe lines are also patterned onto the wafer backside which are etched only half-way through the wafer. Substrate sizes of 3 mm × 4 mm are small enough to be used in a TEM holder. Direct AFM measurements reveal an RMS roughness of less than 1 nm, and no buckling is seen at the window boundaries.

Optical microscopy and ellipsometry

Just as for silicon oxide, the silicon nitride layer affords an extremely smooth and uniform interface that allows for easy calibration of polymer film thickness by the interference colors observed through a microscope. Since the boundary conditions for reflected light are different, these colors are different on the window than off the window for polymer regions of the same thickness (it is straightforward to match these colors by observing regions that extend over the window edge). For 100 nm thick membranes, we find that the interference color contrast from the thinnest polymer regions is typically enhanced on the window areas.

Figure 2a shows results from thin films of symmetric PS-b-PMMA, annealed at 250°C for 24 h. The diblock copolymer contained 53% PS by volume, has an average molecular weight of 65 500, and a polydispersity $M_w/M_n = 1.06$. In bulk, its microphase separates into lamellae with a repeat spacing, L, of 31 nm. The films were prepared by spin-casting the copolymer from a toluene solution onto the substrates and subsequent annealing in an oven with an argon atmosphere. In thin films of lamellar morphology, the polymer prefers its bulk repeat spacing. As a result, the thickness of non-frustrated films usually assumes values that are even or odd half-integer multiples of L, depending on which block covers the substrate and the free surface. Films with nominal thickness not equal to one of these values compensate by separating into flat regions (islands or holes) differing in height by one repeat spacing[2,3]. The inset to *Figure 2a* shows this quantization in a sample with average thickness, $\langle d \rangle$, slightly larger than $3L$. The two height plateaus are clearly delineated by the corresponding, thickness-specific interference colors. AFM measurements confirm that these stable plateaus differ in thickness by 31 nm. By matching the interference colors with ellipsometry data taken on the same film region, we can establish absolute thickness values for the individual plateaus and determine the corresponding integer number, N, of lamellar layers. *Figure 2* shows $\langle d \rangle$, obtained from ellipsometry*, plotted against the average number of lamellar layers, $\langle N \rangle$, for several films. $\langle N \rangle$ was obtained by weighing each integer N with the associated area coverage as calculated from digital image analysis of images like the inset to *Figure 2a*. From the slope, $\partial\langle d \rangle/\partial\langle N \rangle$, of a linear fit to this data we obtain a lamellar repeat spacing $L = (30 \pm 4)$ nm. If the same block wets both interfaces, the quantization condition is $d = NL$, while for asymmetric configurations we have $d = ((2N - 1)/2)L$. Since PS uniformly covers the free

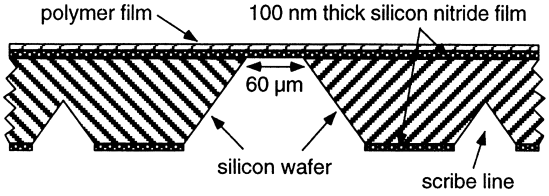

Figure 1 Sketch (not to scale) of a silicon nitride membrane substrate in cross-section with a spun-cast polymer film covering the top

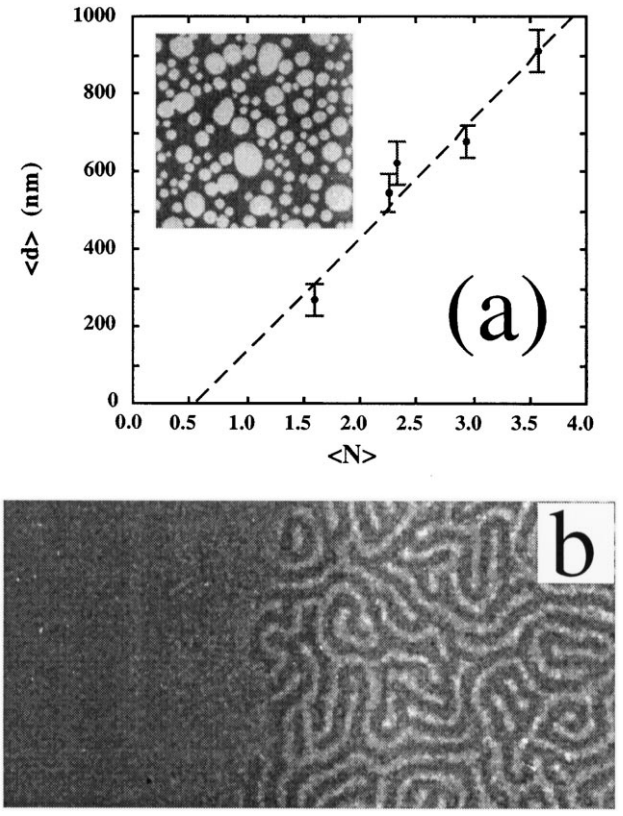

Figure 2 (a) Average film thickness, $\langle d \rangle$, as a function of the average number of repeat spacings, $\langle N \rangle$ for lamellar phase PS-b-PMMA, annealed at 250°C. The inset shows an optical micrograph, of thickness quantization at $\langle d \rangle \approx 3L$, forming $d = \frac{7}{2}L$ islands in a $d = \frac{5}{2}L$ background (field of view 200 μm × 200 μm; the interference colors are converted to gray scale). (b) TEM micrograph near the boundary of a $d = \frac{3}{2}L$ island and a $d = L$ hole, in lamellar PS-b-PMMA annealed at 155°C. Lateral microphase separation occurs in the $d = L$ region. Light domains correspond to PMMA, dark domains to PS (field of view 1 μm × 2 μm)

* Our ellipsometry analysis takes into account the effects of two thin films (polymer and silicon nitride) on a substrate.

surface of PS-b-PMMA films of parallel morphology[2,3], the half-integer intercept of $\langle d \rangle$ with the *x*-axis in *Figure 2a* thus establishes that PMMA wets the silicon nitride substrate.

Combined TEM and AFM imaging

The transparency and stability of the windows makes them highly suitable substrates for combined studies by TEM, which gives information averaged over the film thickness, and AFM, which probes the film surface. Amorphous silicon nitride appears completely featureless under TEM, enabling direct observation by TEM inside the window area, without removing the polymer film. Contrast between PS and PMMA derives from electron beam thinning of the PMMA (which thus appears light in the image)[15], and can be enhanced through heavy metal staining. Our studies were carried out using a Philips CM120 TEM operated at 120 kV. We find that with a silicon nitride thickness of 90–100 nm, excellent TEM contrast is achieved.

One advantage over windowless substrates is the ability to directly observe lateral phase separation by TEM. This is demonstrated in *Figure 2b* for the same lamellar phase diblock as in *Figure 2a*, but annealed for 24 h at 155°C. A new, stable thickness appears at $d = L$ at this lower annealing temperature, due to the particular interfacial wetting properties of PS and PMMA[16]. Lateral phase separation is seen in the $d = L$ thick region on the right. This region is separated by a step boundary from a thicker, $d = \frac{3}{2}L$ region of the usual parallel morphology on the left.

The membranes allow for AFM and TEM imaging at the same film location (*Figure 3a* and *b*). The AFM scans were taken with a Topometrix Discoverer AFM in contact mode. A silicon nitride cantilever was used at an applied force of 1 nN. These images were taken of a PS-b-PMMA diblock copolymer with 66% PS by volume, an average molecular weight of 101 000, and a polydispersity of 1.09. Thin films of this copolymer, spin-cast from solution, form PMMA cylinders parallel to the substrate (repeat spacing 60 nm), surrounded by a PS matrix. In the images shown, domains that appear light in the TEM micrographs (i.e. PMMA

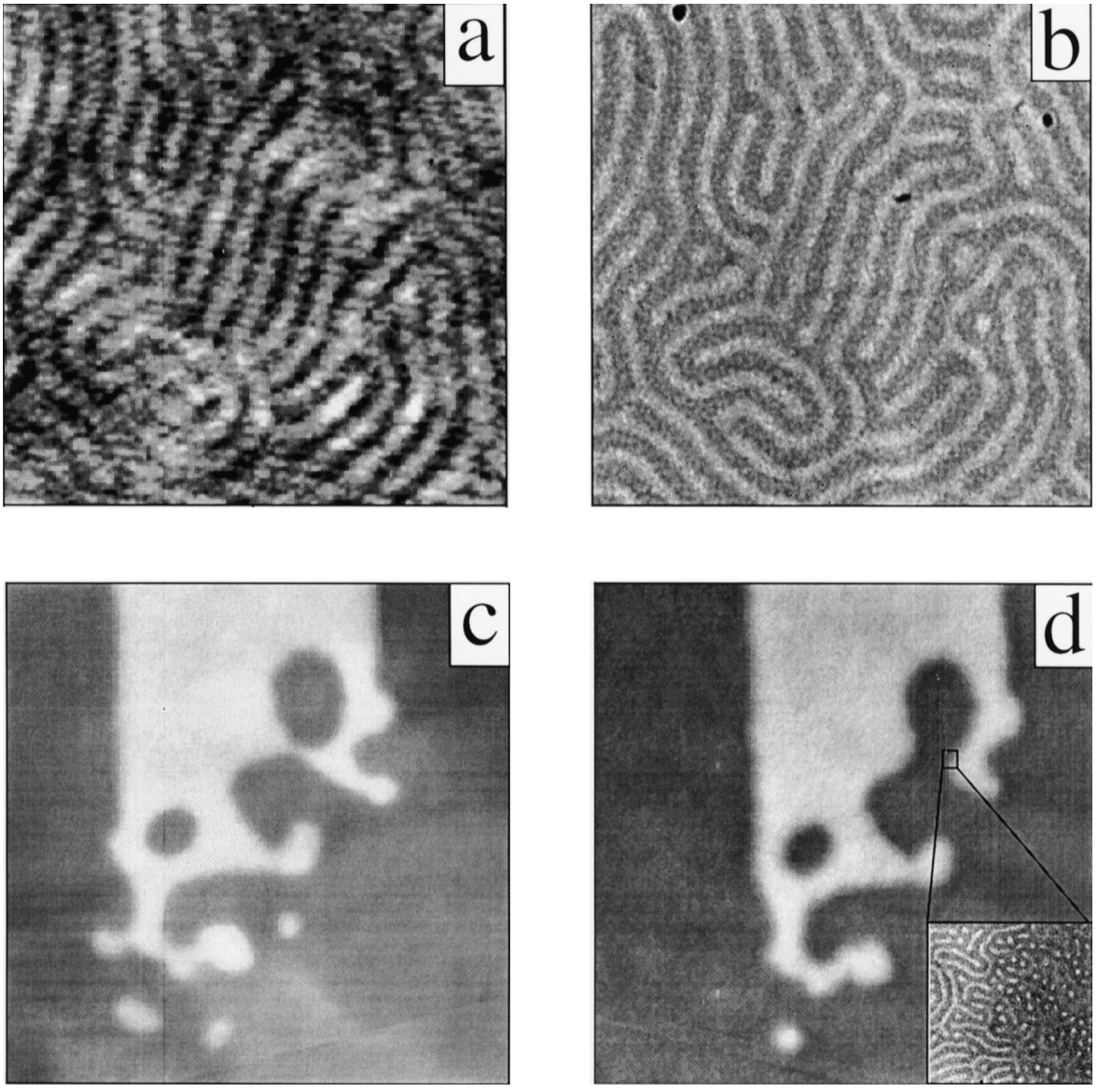

Figure 3 (a) AFM topography (scan rate 1 μm s^{-1}) and (b) TEM image of the identical region (1 μm × 1 μm) of a cylindrical phase PS-b-PMMA thin film. (c) AFM image of the large-scale topography of a PS-b-PMMA thin film 9 h into annealing at 250°C (20 μm × 20 μm image, scan rate 20 μm s^{-1}). (d) Same area after 17 h anneal. The inset shows a TEM close-up of the boxed region

cylinders which have a higher transmissivity) also appear light in the AFM topography images (i.e. are taller). This indicates a corrugated surface with peaks above the cylindrical PMMA domains. This small corrugation (roughly 1 nm, peak to valley) is easily resolved with the AFM and, as shown by *Figure 3a* and *b*, correlates in detail with the local domain configuration observed by TEM. This correlation unambiguously allows AFM images of the surfaces to distinguish between PMMA and PS regions inside the film.

Having established this correlation, we can then use AFM in cases that prohibit the use of TEM. An important example of this kind are *in-situ* investigations of the kinetics associated with terrace formation and thickness quantization in copolymer thin films during annealing. While electron beam exposure alters (e.g. by cross-linking or breaking up) the structure of many polymers, AFM can be non-invasive and thus can be used to track a film's morphological evolution over time. This can be seen in *Figure 3c* and *d* which show the evolution of a large island (plateaus also form in these films) 9 and 17 h into annealing at 250°C. AFM topography scans in this case were performed after quenching to room temperature (well below the glass temperature). Over the 8 h time interval represented by *Figure 3c* and *d* we find that, while the overall island shape has not changed much, most activity has occurred in regions with a high degree of boundary curvature. The thickness of these regions (approximately 5 nm thinner than the more stable plateaus after 9 h anneal), anticipates this rapid change. At the conclusion of an annealing series, a final TEM picture was taken of the same region (inset to *Figure 3d*).

Integration of microfabricated structures

One particular advantage of silicon nitride membrane substrates is that they are rigid enough to allow for simple integration of microfabricated structures such as electrodes or gratings by standard optical or electron-beam lithography. Such structures or patterns can extend over the whole substrate or part of it, without need to avoid the window area. *Figure 4a* shows an image, taken at 45° tilt with a scanning electron microscope (SEM), of a simple set of planar electrodes reaching onto the window area. These electrodes were formed by evaporation of 25 nm of chromium through an electron-beam-patterned resist mask and subsequent lift-off. The polymer film under study can then be spin-cast between such electrodes to allow for either local measurement of electrical film properties over the well-defined area between the electrodes, or for the local application of electric fields. In either case, the membrane allows for subsequent direct TEM investigation of the film morphology between the electrodes.

We have successfully used this technique for electric field alignment of copolymer domains as shown in *Figure 4b*[10]. For this image, a single layer of cylindrical phase PS-b-PMMA was subjected to an electric field $E = 4\ \mathrm{V}\ \mu\mathrm{m}^{-1}$ during a 24 h anneal at 250°C under an inert gas atmosphere, aligning the domains (cf. *Figure 3a* and *b*). By fabricating planar electrodes, we can vary the electric field strength (and orientation) on different regions of the same sample. For high-field applications such as these the large dielectric breakdown strength as well as the high resistivity of silicon nitride is of advantage. Furthermore, by placing the electrode gap region on the membrane, leakage currents through the Si wafer are minimized.

Conclusions

The silicon nitride membrane substrates described here open up new possibilities for multi-technique investigations of organic thin films. In particular, they combine the advantages of solid, semiconductor substrates with the option of direct TEM access to the local film morphology. The examples presented, using PS-b-PMMA thin films, demonstrate the usefulness of the membranes for combining TEM studies with optical microscopy and AFM investigations. The excellent correlation observed between TEM and AFM images will allow for *in-situ* AFM studies to follow the real time kinetics and morphological evolution of thin polymer films. Additional possibilities also exist for micropatterning the substrate prior to film deposition. By combining these methods, measurements of local defect structure dynamics in electric fields are now becoming possible. Silicon nitride membranes should also be useful for investigations of the local morphology induced by steps, trenches, gratings or other structures micropatterned into the substrate surface.

Acknowledgements

We thank P. Infante for assistance with substrate fabrication, E. E. Ehrichs and A. M. Urbas for help with the electron beam lithography, D. Gaspar and B. Isa for assistance with AFM, and T. P. Russell for providing us with the cylindrical phase PS-b-PMMA copolymer. This

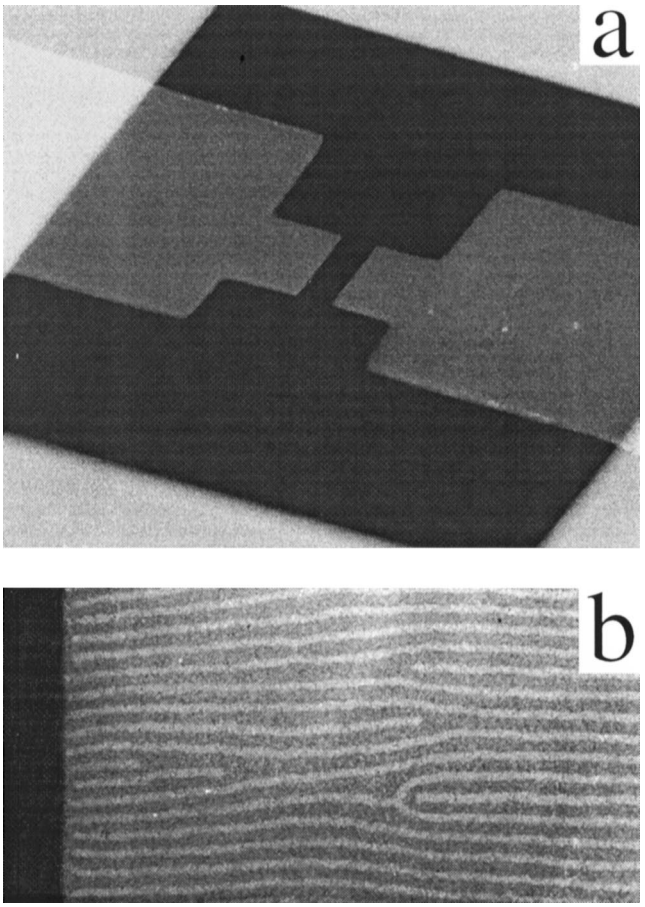

Figure 4 (a) SEM image (taken at 45° tilt) of a set of 25 nm thick Cr electrodes fabricated on top of a membrane. The 60 μm × 60 μm window does not backscatter many electrons and thus appears black in the image. (b) TEM image (1 μm × 2 μm) of electric-field-induced copolymer alignment near an electrode edge (dark bar on left). Light domains correspond to PMMA, dark domains to PS

work was supported in part by the MRSEC program of the National Science Foundation (NSF) under Award No. DMR-9400379, by the Air Force Office of Scientific Research (AFOSR/URI program) and by the David and Lucile Packard Foundation. The silicon nitride membranes were fabricated at the Cornell Nanofabrication Facility, which is supported by NSF under grant ECS-8619049.

References

1. Krausch, G., *Materials Science and Engineering*, 1995, **R14**, 1.
2. Coulon, G., Daillant, J., Collin, B., Benattar, J. J. and Gallot, Y., *Macromolecules*, 1993, **26**, 1582.
3. Coulon, G., Russell, T. P., Deline, V. R. and Green, P. F., *Macromolecules*, 1989, **22**, 2581.
4. Henkee, C. S., Thomas, E. L. and Fetters, L. J., *Journal of Materials Science*, 1988, **23**, 1685.
5. Kunz, M. and Shull, K., *Polymer*, 1993, **34**, 2427.
6. Menelle, A., Russell, T. P., Anastasiadis, S. H., Satija, S. K. and Majkrzak, C. F., *Physical Review Letters*, 1992, **68**, 67.
7. Annis, B. K., Schwark, D. W., Reffner, J. R., Thomas, E. L. and Wunderlich, B., *Makromol. Chem.*, 1992, **193**, 2589.
8. Kellogg, G. J., Walton, D. G., Mayes, A. M., Lambooy, P., Russell, T. P., Gallagher, P. D. and Satija, S. K., *Physical Review Letters*, 1996, **76**, 2503.
9. Krausch, G., Kramer, E. J., Rafailovich, M. and Sokolov, J., *Appl. Phys. Lett.*, 1994, **64**, 2655.
10. Morkved, T. L., Lu, M., Urbas, A. M., Ehrichs, E. E., Jaeger, H. M., Mansky, P. and Russell, T. P., *Science*, 1996, **273**, 931.
11. Green, E. D. and Kino, G. S., *Journal of Vacuum Science and Technology B*, 1991, **9**, 1557.
12. Ralls, K. S. and Buhrman, R. A., *Physical Review Letters*, 1988, **60**, 2434.
13. Casey, S., Hill, E., Miles, J., Sivasamy, P., Birtwistle, K., Middleton, B., Chapman, J. and Rose, J., *J. Magnetism Magnetic Mats.*, 1996, **155**, 348.
14. Kendall, D. L., *Annual Review of Material Science*, Vol. 9. Annual Reviews, Palo Alto, California, 1979, p. 373.
15. Thomas, E. L. and Talmon, Y., *Polymer*, 1978, **19**, 225.
16. Morkved, T.L. and Jaeger, H.M., *Europhys. Let*,, 1997, **40**, 643.